Bulletin of Electrical Engineering and Informatics
Vol. 13, No. 3, June 2024, pp. 1594~1601
ISSN: 2302-9285, DOI: 10.11591/eei.v13i3.6789

Low insertion loss open-loop resonator–based microstrip diplexer with high selective for wireless applications

Rania Hamdy Elabd[1], Ahmed Jamal Abdullah Al-Gburi[2], Khaled Alhassoon[3], Mohd Muzafar Ismail[2], Zahriladha Zakaria[2]
[1]Department Electronic and Communication, Higher Institute of Engineering and Technology in New Damietta, Damietta, Egypt
[2]Centre of Telecommunication Research and Innovation, Faculty of Electronics and Computer Technology and Engineering, Universiti Teknikal Malaysia Melaka, Melaka, Malaysia
[3]Department of Electrical Engineering, College of Engineering, Qassim University, Unaizah, Saudi Arabia

Article Info

Article history:

Received May 24, 2023
Revised Oct 2, 2023
Accepted Oct 24, 2023

Keywords:

Band pass filter
Selectivity
Insersion loss
Microstrip diplexer
Open loop resonator

ABSTRACT

This paper presents a low-insertion-loss open-loop resonator (OLR)-based microstrip diplexer with high-selective for wireless applications. We used two series capacitive gaps in the microstrip transmission line, loaded with rectangular-shaped half-wavelength OLRs, to create a high-selectivity bandpass filter (BPF). The planned BPFs are linked through a T-junction combiner, precisely tuned to align with both filters and the antenna port in order to produce the proposed diplexer. The system is implemented on a rogers TMM4 substrate with a loss tangent of 0.002, a dielectric constant of 4.7, and a thickness of 1.52 mm. The suggested diplexer has dimensions of (90×70) mm². It achieves a modest frequency space ratio of R=0.1646 in both transmit and receive modes by having two resonance frequencies of ft=2.191 GHz and fr=2.584 GHz, respectively. The simulated structure displays good insertion losses of approximately 1.2 dB and 1.79 dB for the two channels, respectively, at fractional bandwidths of 1.24% at 2.191 GHz and 0.636% at 2.584 GHz. The simulated isolation values for 2.191 GHz and 2.584 GHz are 53.3 dB and 66.5 dB, respectively.

Corresponding Author:

Zahriladha Zakaria
Center for Telecommunication Research and Innovation
Faculty of Electronics and Computer Technology and Engineering, Universiti Teknikal Malaysia Melaka
Melaka, Malaysia
Email: zahriladha@utem.edu.my

1. INTRODUCTION

In the last few years, wireless communication technologies are essential and play a significant part in many wireless system applications [1]. A key component of frequency division duplex technology is the microwave diplexer [2], [3]. Three-port devices are called diplexers. The diplexer devices divide the input signal from the single input port into two distinct channels that operate at two different desirable frequencies [4]–[6]. A variety of microstrip diplexer types are introduced. Unfortunately, they all take up a lot of space [7]–[23]. A cavity-backed self-diplexing Y-shaped slot antenna utilizing quarter-mode substrate integrated waveguide (QMSIW) is designed for achieving high isolation [7]. This antenna incorporates a Y-shaped slot on the top surface of the rectangular substrate integrated waveguide (SIW), creating two unequal radiating openings for transmitting signals at both 3.9 GHz and 4.9 GHz frequencies. While this configuration results in a high-gain antenna, it suffers from poor transmission-reception isolation at 34 dB and a relatively wide frequency separation, with a space ratio of r=0.227. A self-diplexing bow-tie shaped slot antenna is introduced, which is based on a SIW cavity [8]. This design excites the SIW cavity using two distinct feed lines, causing it to resonate at the frequencies used for transmission, and reception. This well-known setup produces a high-gain antenna with a unidirectional radiation pattern. However, it still exhibits a substantial frequency space ratio of r=0.22 and suboptimal transmission-reception isolation at 22 dB. Feng *et al.* [9] combine the global system for mobile (GSM) and wireless local area network (WLAN) frequency bands using a microstrip diplexer. The negative effects of the microstrip diplexer are reduced by this design. It has some shortcomings, such as significant channel losses and a 30 dB isolation limit. A straightforward method for designing a microstrip diplexer is suggested in [10]. It is built using two small square open loop resonator band pass filters together. These filters were created for 2.45 GHz radio frequency identification applications. Chebychev's approximation is used. Diplexer isolation is 40 dB. A dual-mode resonator-based substrate integrated waveguide (SIW) diplexer is suggested in [11]. This diplexer is used to enhance RF front end performance. This diplexer provides appropriate isolation of 49 dB and 53 dB, respectively, for the broadcast and receive channels. Yet, some of its shortcomings are its size. A squared open-loop resonator (SOLR)-based microstrip diplexer is proposed in [12] for implementation. The suggested diplexer achieves a tiny frequency space ratio of R=0.114 and has two resonance frequencies of 1.81 GHz and 2.03 GHz for the transmit and receive channels, respectively. Yet, some of its shortcomings are its size.

A microstrip diplexer has been created by combining two separate channel filters to a dual-band bandpass filter [13]. This design avoids the requirement for external junctions in the construction of diplexers, in contrast to the conventional design method that necessitates separate connections or junctions for energy distribution. A 50 dB isolation between the diplexer's broadcast and receive bands was shown by simulation results and experimental observations. Nonetheless, it did have significant insertion losses in the transmit and receive bands of 2.88 dB and 2.95 dB, respectively. A brand-new microstrip diplexer with good isolation and selectivity has been presented in [14]. It is based on combining two small-size bandpass filters composed of open/shorted lines and an open stub for LTE applications. For the frequency response performance to be improved, many types of resonators are used [15]–[27]. Recently, other resonator shapes such as u-shaped [15], [16], t-shaped [17], pi-shaped [18], stepped-impedance [19], and patch resonators [20], [21] have been introduced, showcasing the diverse and innovative approaches in the field of resonator design for various applications in electronics and communication systems. Patch resonators are utilized in [22] to produce a filtering response. In order to create a microstrip diplexer, two bandpass filters (BPFs) made of spiral cells and coupled lines are integrated in [23]. It has some drawbacks, including unwanted harmonics and large losses at both channels. The layout arrangement of the demonstrated microstrip diplexer in [24] uses three coupled lines structures to better reduce harmonics, however the issue of large losses at both channels is still present. While efforts are being made to create a compact microstrip bandpass diplexer with good performance, the design aspects, such as low losses and increased fractional bandwidth, make it difficult to sacrifice the compact size.

This work introduces a high isolation and low insertion loss effective design scheme for microstrip diplexers. The two compact size BPFs that make up the proposed diplexer are constructed from linked OLRs. A T-junction that serves as a combining circuit connects the two BPFs to the antenna and provides good isolation between the up-link and down-link BPFs. Initially, a high selectivity BPF is created for 2.191 GHz operation. The suggested microstrip diplexer is then made up of the other BPF, which is created to operate at 2.584 GHz, and the first BPF.

2. PROPOSED OLR-BASED MICROSTRIP DIPLEXER

Generally, two band pass filters are constructed as the initial step in the microstrip diplexer design process. In this part, a different design for a highly effective microstrip diplexer operating at $f_t = 2.191\ GHz$ and $f_r = 2.584\ GHz$ for transmit and receive modes, respectively, is shown using the computer simulation technology (CST) software.

The specified rogers TMM4 substrate has the planned diplexer printed on both sides of it. In order to achieve the desired, transmit, and receive frequencies, $f_t = 2.191\ GHz$ and $f_r = 2.584\ GHz$, respectively, two selective BPFs are joined together to form the proposed diplexer. The T-junction is used to join the two BPFs together. As a result, the suggested diplexer's design process can be completed in the following two steps: i) the transmit and receive BPF designs and ii) the planned microstrip diplexer's meeting.

2.1. Creating the transmit and receive bandpass filters

In this section, we introduce designs for the transmit and receive bandpass filters (BPFs). The proposed topology for the microstrip bandpass filter is shown in Figure 1. As is evident, this structure comprises two input/output feed lines and a typical rectangular open-loop resonator. The separation L_f serves to separate the two feed lines, whereas gap g_1 facilitates coupling between the two transmission lines and the resonator. In this instance, a better size reduction is guaranteed by the folded microstrip resonator and the efficient placement of the two feed lines. CST-MWS-2019 was used to investigate the operation of the BPF and simulate the shown OLR-BPF, which are printed on a 1.52 mm rogers TMM4 substrate.

At the transmit frequency of $f_t = 2.191\ GHz$, OLRs are used, as shown in Figures 1(a) and (b), each with a total length of roughly $\lambda_g/2$. Table 1 contains a list of the filter's dimensions. The width and length of the trace line, coupled with the separation gap g_1, determine each resonator's internal capacitance, which in turn influences the filter's selectivity and insertion loss.

Figure 1(c) illustrates the simulated scattering parameters for the proposed transmit bandpass filter, as determined through CST microwave studio. This filter features a central frequency of 2.191 GHz, a 3 dB bandwidth spanning 47.1 MHz, a fractional bandwidth of 1.24%, a return loss of 20 dB, and an insertion loss of 1.4 dB, successfully meeting various performance requirements. The suggested receive BPF, which has dimensions indicated in Table 1, is depicted in Figures 2(a) and (b) and follows the same conceptual framework. Figure 2(c) displays the receive BPF's simulated scattering parameters. The curves analysis reveals the BPF's center frequency to be 2.584 GHz, 3dB bandwidth to be 20.7 MHz, fractional bandwidth to be 0.636%, return loss to be 15.6 dB, and insertion loss to be 1.3 dB.

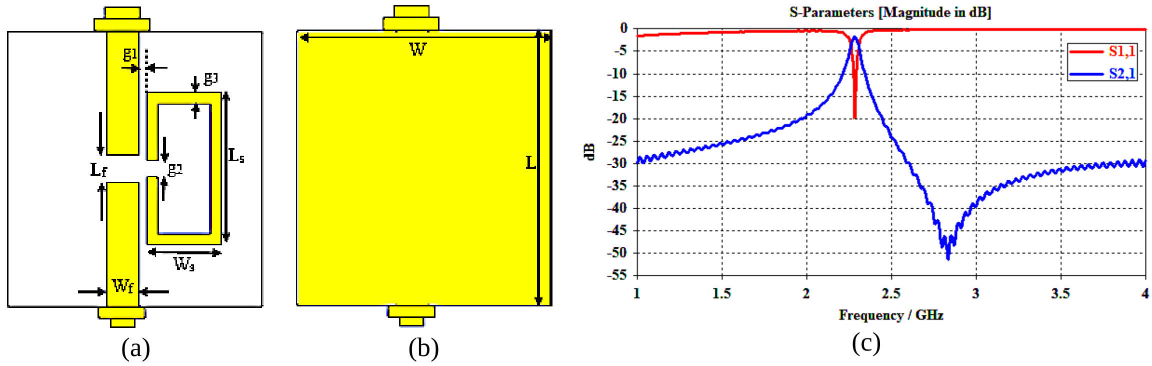

Figure 1. Depicts the geometric design of the transmit bandpass filter based on OLR, featuring a resonance frequency of f_t=2.191 GHz; (a) presents the top view, while (b) provides the bottom view, and (c) the receive BPF's simulated S-parameters

Table 1. The suggested transmit and receive BPF's dimensions

Parameter	Value (mm)	Parameter	Value (mm)
W	25	L_{s1}	11.2
L	25	g_1	0.75
W_f	3.06	g_2	1.5
L_f	2.5	g_3	1
W_s	7	g_{s1}	0.75
L_s	14	g_{s2}	1.75
W_{s1}	7	g_{s3}	1

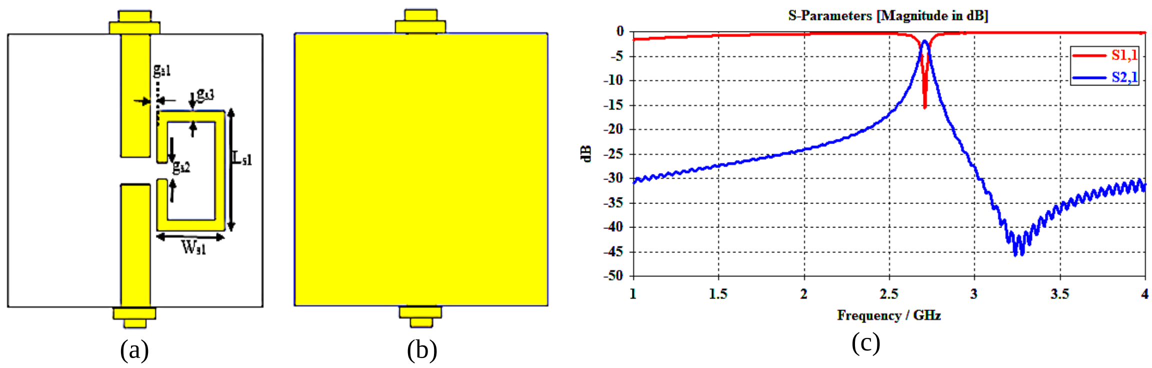

Figure 2. The geometrical construction of the OLR-based receive BPF with resonance frequency $f_t = 2.584\ GHz$; (a) top view, (b) bottom view, and (c) the transmit BPF's simulated S-parameters

The second method in this section is committed to studying the proposed approach by changing the microstrip design to its corresponding tuned circuit (LC) model, as illustrated in Figure 3. This conversion is performed to gain a better understanding of the behavior of the suggested BPF. The suggested topology is symmetric, making it simple to use half circuit LC analysis to convert the microstrip transmission lines to the LC model, as illustrated in Figure 3. The microstrip transmission lines are assumed to have negligible losses, and the LC model used is an approximation. In this LC model, the inductance of the central transmission lines is approximated using parameters L1 to L9C1 addresses the capacitance arising from the space between the two feed lines, whereas C2 and C3 simulate the capacitance effects that stem from the gap between the feed line and the resonator. C8 and C9 depict the capacitance effects of the open stubs with respect to the ground, and the capacitance effects resulting from the bends are also symbolized by values C3, C4, C5, and C6.

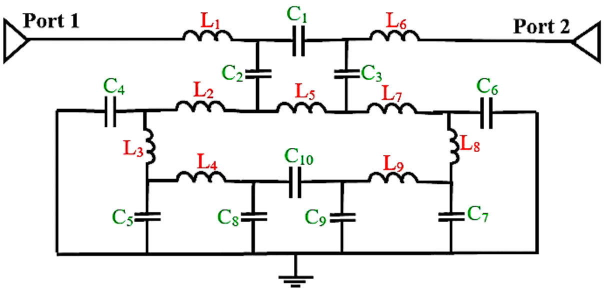

Figure 3. The proposed BPF's LC equivalent circuit

Every component of the microstrip line is then modified to an equivalent LC component after being divided into smaller sections to assist the conversion process. The electrical magnitudes of each element are determined using the calculation method provided in [25].

The effective dielectric constant and the characteristic impedance are the two primary parameters that should be determined, therefore for a line width $\mathrm{W_f} = 3.06\ mm$, we obtain ($\varepsilon_{\mathrm{re}} = 3.55$, $Z_c = 49.9$). The modified circuit is then simulated in a schematic environment, following the use of the calculating procedure several simulations were conducted, wherein adjustments were made to the values of individual LC model components to improve the alignment between electromagnetic simulation results and the converted circuit. The LC equivalent circuit of the proposed BPF was simulated using the electromagnetic simulator ADS. The simulated scattering parameters of the LC model using the ADS simulation tool are shown in Figure 4. It is noticed that the behavior of the BPFs is ideal and allows to pass frequency 2.191 GHz (Figure 4(a)) at values of the LC components as follow: $L_1 = 0.01$, $L_2 = 0.01$, $L_3 = 0.01$, $L_4 = 0.01$, $L_5 = 0.01$, $L_6 = 0.01$, $L_7 = 0.009$, $L_8 = 0.01$, $L_9 = 0.01$ (all in nH). $C_1 = 4.2, C_2 = 1\mathrm{e}-6$, $C_3 = 0.18$, $C_4 = 1\mathrm{e}-6$, $C_5 = 0.12$, $C_6 = 0.12$, $C_7 = 0.15$, $C_8 = 7.4$, $C_9 = 6$, $C_{10} = 0.12$ (all in pF), and 2.584 GHz (Figure 4(b) at values of the LC components as follow: $L_1 = 0.01$, $L_2 = 0.01$, $L_3 = 0.01$, $L_4 = 0.01$, $L_5 = 0.01$, $L_6 = 0.01$, $L_7 = 0.009$, $L_8 = 0.01$, $L_9 = 0.01$ (all in nH). $C_1 = 4.8, C_2 = 1\mathrm{e}-6$, $C_3 = 0.17$, $C_4 = 1\mathrm{e}-6$, $C_5 = 1\mathrm{e}-6$, $C_6 = 8.6$, $C_7 = 1.4$, $C_8 = 7.4$, $C_9 = 6$, $C_{10} = 0.12$ (all in pF).

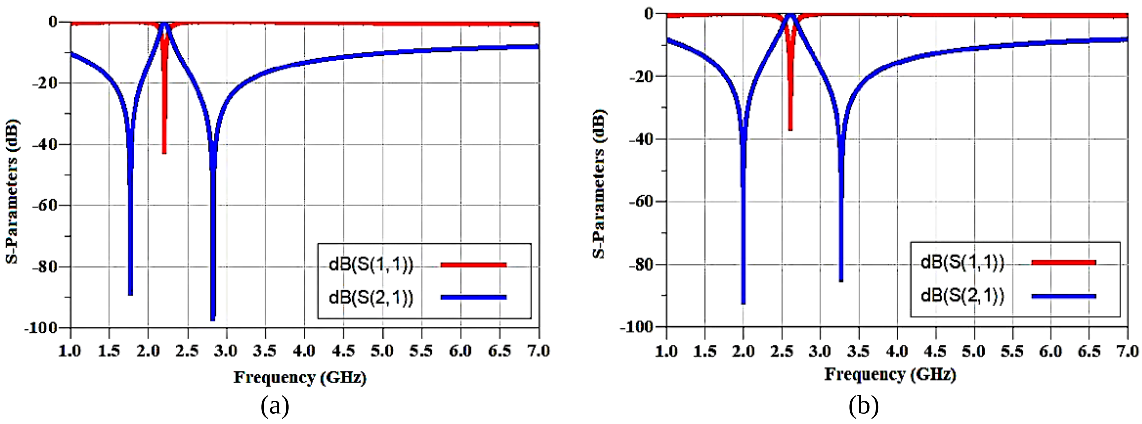

Figure 4. Scattering parameter of proposed BPF equivalent circuit in ADS simulation program; (a) at 2.191 GHz and (b) at 2.584 GHz

2.2. The suggested microstrip diplexer's assembly

The two OLR-based BPFs discussed before and shown in subsection 2.1 are connected by a T-junction in this section to introduce the whole configuration of the proposed diplexer as shown in Figure 5, where Figure 5(a) is top view and Figure 5(b) is bottom view. The isolation among transmit and receive channels is controlled by the width and length of the T-junction branches. Table 2 has a list of the proposed diplexer's dimensions.

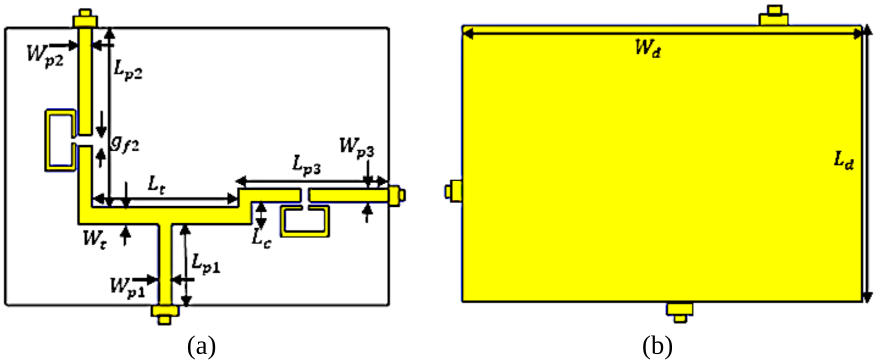

Figure 5. The suggested diplexer's construction; (a) top view and (b) bottom view

Table 2. The suggested diplexer's dimensions

Parameter	Value (mm)	Parameter	Value (mm)
W_d	90	W_{p2}	3.065
L_d	70	L_{p2}	41.2
W_{p1}	3.056	W_{p3}	3.065
L_{p1}	25	L_{p3}	32
W_t	405	g_{f2}	2.5

Figure 6 displays the simulation results of the proposed diplexer's scattering parameters $|S_{11}|$,$|S_{21}|$, and $|S_{31}|$ versus frequency. For the transmit and receive channels, respectively, the structure displays good insertion losses of around 1.2 dB and 1.7 dB, with fractional bandwidths of 1.24% at $f_t = 2.191\ GHz$ and 0.636% at $f_r = 2.584\ GHz$. To put it another way, the transmit and receive bands' respective 3dB bandwidths are 36 MHz and 21.1 MHz, and the corresponding simulated return losses are 40 dB and 26 dB. The scattering parameter $|S_{32}|$ is displayed in Figure 7. The simulated isolation values are 53.3 dB and 66.5 dB, respectively, at 2.191 GHz and 2.584 GHz. The suggested diplexer also achieves a modest frequency space ratio R=0.1646. This ratio is defined as the distance among the transmit and receive frequencies $\Delta f = |f_r - f_t|$ and the center of frequency $f_c = (f_t + f_r)/2$, where R is given by [26].

$$R = \Delta f / f_c \tag{1}$$

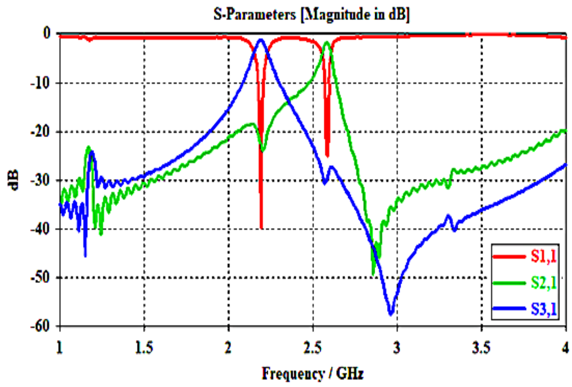

Figure 6. The suggested diplexer's simulated S-parameters

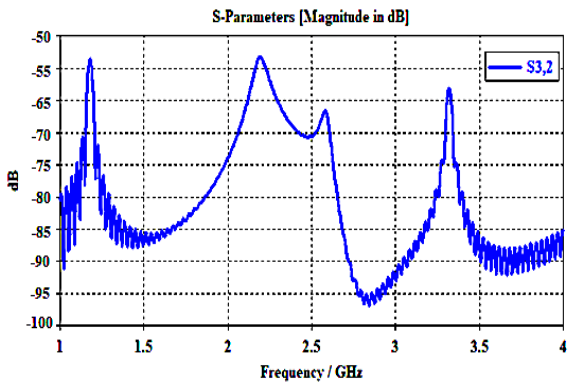

Figure 7. The suggested diplexer's simulated scattering parameter $|S_{32}|$

Figure 8 displays the proposed diplexer's simulated current distributions at transmit and receive frequencies. As depicted in Figure 8(a), the transmission line connecting port 1 to port 3 exhibits a significant current density when the diplexer is set to transmit at a frequency of f_t=2.191 GHz, while the connection from port 1 to port 2 is effectively an open circuit. Conversely, in Figure 8(b), when the diplexer operates at the receiving frequency f_r=2.584 GHz, the line between port 1 and port 2 displays high current density, and the path between port 1 and port 3 is essentially an open circuit. This results in strong isolation between the broadcasting and receiving channels.

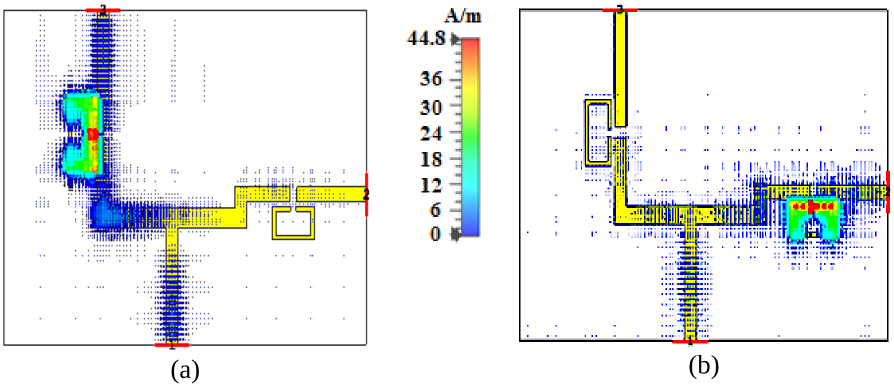

Figure 8. Distribution of surface current in the suggested diplexer at; (a) $f_t = 2.191\ GHz$, and (b) $f_r = 2.584\ GHz$

The suggested diplexer has a good properties and performance in terms of dimention, resonance frequency (GHz) at transmit channel and receive channel, fractional bandwidths (FBW (GHz)), insertion loss (dB), return loss (dB), isolation (dB), and frequency space ratio (R), compared to #1 up to #15. A comparison displays a competitive version of the offered diplexer designs, which are organized in Table 3.

Table 3. Comparison with related work

#	Ref.	Size λ_g^2	Frequency (GHz)	FBW (%)	Insertion loss (dB)	Return loss (dB)	Isolation (dB)	R
1	[5]	0.0233	1.7/3.3	1.8	0.87	-36	-23/-25	0.64
2	[7]	0.6889	3.9/4.9	NA	NA	-32/-38	-34	0.227
2	[8]	0.4356	9/11.2	NA	NA	-28/-32	-25	0.22
4	[9]	0.35	1.8/2.4	6/5.8	NA	-23/-25	30	0.286
5	[10]	1.2	2.2/2.6	4.55/5	1.6/1	-20	40	0.167
6	[11]	4.6	8.04/9.07	4.23/4.19	2.35/2.33	-22/-30	49/53	0.12
7	[12]	1.5	1.81/2.03	2.25/3	1.98/1.9	-30/-38	58/46	0.114
8	[14]	0.167	1.8/2.1	5.5/6.2	2/1.8	-28/-30	40	0.154
9	[22]	0.89	1.85/2.5	NA	4.2/3.3	-20/-19	31	NA

3. CONCLUSION

This article presents a highly effective microstrip diplexer for a wireless communication system using OLR BPFs, which achieves excellent selectivity, strong isolation, a minimal frequency gap, and minimal insertion loss. It operates at $f_t = 2.191$ GHz and $f_r = 2.584$ GHz, and Roger TMM4 has been selected as the substrate due to its minimal electrical loss and steady dielectric constant across frequency. The suggested design of the diplexer has been designed employing CST microwave studio software, demonstrating the best performance with high isolation of approximately 53.3 dB and 66.5 dB for 2.191 GHz and 2.584 GHz, respectively. It also demonstrates the lowest insertion loss of approximately 1.2 dB for the transmit channel and 1.7 dB for the receive channel, as well as an acceptable frequency space ratio of approximately 0.1646 and small fractional bandwidths of 1.24% and 0.636% for the transmit and receive channels, respectively. A numerical equation for the LC equivalent circuit of the recommended BPF and the suggested microstrip diplexer was built. The finalized diplexer is well suited for wireless communication systems due to its miniaturized size, minimal insertion loss, and great selectivity.

ACKNOWLEDGEMENTS

The authors express their gratitude to Universiti Teknikal Malaysia Melaka (UTeM), the Ministry of Higher Education (MOHE), and the Higher Institute of Engineering and Technology in New Damietta, Egypt for their assistance in this research.

REFERENCES

[1] J. Zhou, D. Qiao, and H. Qian, “Virtual full-duplex buffer-aided relay selection schemes for secure cooperative wireless networks,” *Eurasip Journal on Wireless Communications and Networking*, vol. 2022, no. 1, p. 44, Dec. 2022, doi: 10.1186/s13638-022-02127-1.

[2] L. Zhou, W. Zhou, Y. Sun, Y. Han, J. Jiang, and D. Zhang, “Design of High-Order Resonator HTS Diplexer with Very Different FBW,” *Electronics (Switzerland)*, vol. 12, no. 3, p. 691, Jan. 2023, doi: 10.3390/electronics12030691.

[3] M. A. E. Eid *et al.* "Highly Efficient GaN Doherty Power Amplifier for N78 Sub-6 GHz Band 5G Applications," *Electronics* , 12, 2023, doi: 10.3390/electronics12194001.

[4] R. J. Wenzel, “Printed-Circuit Complementary Filters for Narrow Bandwidth Multiplexers,” *IEEE Transactions on Microwave Theory and Techniques*, vol. MTT-16, no. 3, pp. 147–157, 1968, doi: 10.1109/TMTT.1968.1126635.

[5] A. J. A. Al-Gburi, I. B. M. Ibrahim, M. Y. Zeain, and Z. Zakaria, “Compact Size and High Gain of CPW-Fed UWB Strawberry Artistic Shaped Printed Monopole Antennas Using FSS Single Layer Reflector,” *IEEE Access*, vol. 8, pp. 92697–92707, 2020, doi: 10.1109/ACCESS.2020.2995069.

[6] A. Chinig, “Review on Technologies used to Design RF Diplexers,” *International Journal of Biosensors & Bioelectronics*, vol. 4, no. 1, p. 23–25, 2018, doi: 10.15406/ijbsbe.2018.04.00091.

[7] A. A. Althuwayb, “Design of highly compact self-diplexing Y-shaped slot antenna employing quarter-mode substrate integrated waveguide,” *International Journal of RF and Microwave Computer-Aided Engineering*, vol. 31, no. 10, 2021, doi: 10.1002/mmce.22827.

[8] S. Mukherjee and A. Biswas, “Design of self-diplexing substrate integrated waveguide cavity backed slot antenna,” *IEEE Antennas and Wireless Propagation Letters*, vol. 15, pp. 1775–1778, 2016.

[9] W. Feng, X. Gao, and W. Che, “Microstrip diplexer for GSM and WLAN bands using common shorted stubs,” *Electronics Letters*, vol. 50, no. 20, pp. 1486–1488, Sep. 2014, doi: 10.1049/el.2014.2500.

[10] H. Tizyi, F. Riouch, A. Tribak, A. Najid, and A. Mediavilla, “Microstrip diplexer design based on two square open loop bandpass filters for RFID applications,” *International Journal of Microwave and Wireless Technologies*, vol. 10, no. 4, pp. 412–421, May 2018, doi: 10.1017/S1759078718000314.

[11] F. Cheng, C. Gu, B. Zhang, Y. Yang, and K. Huang, “High Isolation Substrate Integrated Waveguide Diplexer with Flexible Transmission Zeros,” *IEEE Microwave and Wireless Components Letters*, vol. 30, no. 11, pp. 1029–1032, 2020, doi: 10.1109/LMWC.2020.3025698.

[12] M. M. Shaheen, N. M. Mahmoud, M. A. Ali, M. E. Nasr, and A. H. Hussein, “Implementation of a Highly Selective Microstrip Diplexer with Low Insertion Loss Using Square Open-Loop Resonators and a T-Junction Combiner,” *Radioengineering*, vol. 31, no. 3, pp. 357–361, 2022, doi: 10.13164/RE.2022.0357.

[13] A. O. Nwajana and K. S. K. Yeo, “Microwave diplexer purely based on direct synchronous and asynchronous coupling,” *Radioengineering*, vol. 25, no. 2, pp. 247–252, Apr. 2016, doi: 10.13164/re.2016.0247.

[14] W. Feng, M. Hong, and W. Che, “Microstrip diplexer design using open/shorted coupled lines,” *Progress in Electromagnetics Research Letters*, vol. 59, pp. 123–127, 2016, doi: 10.2528/PIERL16030805.

[15] G. Karimi, A. Lalbakhsh, K. Dehghani, and H. Siahkamari, “Analysis of novel approach to design of ultra-wide stopband microstrip low-pass filter using modified U-shaped resonator,” *ETRI Journal*, vol. 37, no. 5, pp. 945–950, 2015, doi: 10.4218/etrij.15.0114.0188.

[16] A. Lalbakhsh, M. U. Afzal, K. P. Esselle, and S. L. Smith, “An array of electromagnetic bandgap resonator antennas for v-band backhaul applications,” *The International Institute of Engineers and Researchers*, pp. 69–71, 2019.

[17] H. Sariri, Z. Rahmani, A. Lalbakhsh, and S. Majidifar, “Compact LPF using t-shaped resonator,” *Frequenz*, vol. 67, no. 1–2, pp. 17–20, 2013, doi: 10.1515/freq-2012-1043.

[18] Z. Wang and C. W. Park, “Multiband pi-shaped structure with resonators for tri-band wilkinson power divider and tri-band rat-race coupler,” *IEEE MTT-S International Microwave Symposium Digest*, vol. 1, no. 7–22, pp. 1–3, 2012, doi: 10.1109/MWSYM.2012.6259462.

[19] K. Dehghani, G. Karimi, A. Lalbakhsh, and S. V. Maki, “Design of lowpass filter using novel stepped impedance resonator,” *Electronics Letters*, vol. 50, no. 1, pp. 37–39, 2014, doi: 10.1049/el.2013.3144.

[20] Q. Zhang, G. Zhang, Z. Liu, W. Chen, and W. Tang, “Dual-Band Filtering Power Divider Based on a Single Circular Patch Resonator with Improved Bandwidths and Good Isolation,” *IEEE Transactions on Circuits and Systems II: Express Briefs*, vol. 68, no. 11, pp. 3411–3415, 2021, doi: 10.1109/TCSII.2021.3081266.

[21] S. Chen, S. Qi, X. Chen, G. Sun, and W. Wu, “Five-way radial filtering power divider using back-to-back quarter-mode substrate-integrated waveguide and microstrip resonator,” *Electronics Letters*, vol. 57, no. 23, pp. 888–890, 2021, doi: 10.1049/ell2.12299.

[22] H. A. Hussein, Y. S. Mezaal, and B. M. Alameri, “Miniaturized microstrip diplexer based on fr4 substrate for wireless communications,” *Elektronika ir Elektrotechnika*, vol. 27, no. 5, pp. 34–40, 2021, doi: 10.5755/j02.eie.28942.

[23] C. F. Chen *et al.*, “Design of Microstrip Multifunction Integrated Diplexers with Frequency Division, Frequency Selection, and Power Division Functions,” *IEEE Access*, vol. 9, pp. 53232–53242, 2021, doi: 10.1109/ACCESS.2021.3070319.

[24] S. I. Yahya, A. Rezaei, and L. Nouri, “Compact wide stopband microstrip diplexer with flat channels for WiMAX and wireless applications,” *IET Circuits, Devices and Systems*, vol. 14, no. 6, pp. 846–852, 2020, doi: 10.1049/iet-cds.2020.0010.

[25] A. Chinig, A. Errkik, L. El Abdellaoui, A. Tajmouati, J. Zbitou, and M. Latrach, “Design of a microstrip diplexer and triplexer using open loop resonators,” *Journal of Microwaves, Optoelectronics and Electromagnetic Applications*, vol. 15, no. 2, pp. 65–80, Jun. 2016, doi: 10.1590/2179-10742016v15i2602.

[26] A. H. Hussein, H. H. Abdullah, M. A. Attia, and A. M. Abada, “S-Band compact microstrip full-duplex Tx/Rx patch antenna with high isolation,” *IEEE Antennas and Wireless Propagation Letters*, vol. 18, no. 10, pp. 2090–2094, Oct. 2019, doi: 10.1109/LAWP.2019.2937769.

[27] X. J. Lin, Z. M. Xie, and P. S. Zhang, “Small transmit-receive frequency space filtering duplex patch antenna array with high isolation,” *Progress In Electromagnetics Research C*, vol. 71, pp. 161–168, 2017, doi: 10.2528/PIERC16120603.

BIOGRAPHIES OF AUTHORS

Rania Hamdy Elabd received her Ph.D. degree from the Department of Electronics and Communications Engineering, Mansoura University, Egypt in 2020. She received her M.Sc. from the Department of Electronics and Communications Engineering, Mansoura University, Egypt in 2013 and the B.Sc. degree in Electronics and Communications Engineering from the Faculty of Engineering-Mansoura University-Egypt by 2008. She worked as a lecturer at new Damietta Higher Institute of Engineering and Technology-Egypt. Her current research interests are in wireless communication systems, design and optimization of microstrip antennas, and their applications. She has many published papers in communication field. She can be contacted at email: eng.rania87@yahoo.com.

Ahmed Jamal Abdullah Al-Gburi received his M.Eng. and Ph.D. degrees in Electronics and Computer Engineering (Telecommunication Systems) from Universiti Teknikal Malaysia Melaka (UTeM), Malaysia, in 2017 and 2021, respectively. He is currently a senior lecturer at the Faculty of Electrical and Electronic Engineering Technology (FTKEE). From December 2021 to March 2023, he served as a postdoctoral fellow with the microwave research group (MRG) at UTeM. In 2022, he was recognized as one of the top 2% scientists worldwide by Stanford University and published by Elsevier. He has authored and co-authored numerous journal articles and conference proceedings. His research interests encompass microwave sensors, metasurfaces, UWB antennas, array antennas, and miniaturized antennas for UWB and 5G applications. He has been awarded the Best Paper Award from the IEEE Community and has earned several gold, silver, and bronze medals in international and local competitions. He can be contacted at email: ahmedjamal@ieee.org.

Khaled Alhassoon received Bachelor of Science (B.Sc.) degree from Qassim University in 2011. He received a Master of Science (M.Sc.) degree from Drexel University in 2016. He received his Ph.D. from Drexel University on the topic of Magnetically Tuned 3D-printed antenna arrays in 2020. He also worked as a teacher assistant from 2012-2013 at Qassim University. He is currently working as Assistant Professor of Electrical Engineering of the Engineering College at Qassim University. His current research interests include electromagnetics, antennas applications, biomedical applications, and nanotechnology. He can be contacted at email: k.hassoon@qu.edu.sa.

Mohd Muzafar Ismail received his Ph.D. in Atmospheric Discharges from Uppsala University in Sweden under the supervision of Prof. Vernon Cooray. His present research interest focuses on atmospheric discharges and specifically lightning safety. He is graduate member and professional engineer with the Board of Engineers of Malaysia. Presently, he is active in teaching, consulting and research in the field of lightning and electronics. He can be contacted at email: jeefferie@utem.edu.my.

Zahriladha Zakaria received the B.Eng. and M. Eng in Electrical and Electronic Engineering from the University Teknologi Malaysia in 1998 and 2004 respectively, and the Ph.D. degree in Electrical and Electronic Engineering from the Institute of Microwaves and Photonics (IMP), University of Leeds, United Kingdom in 2010. From 1998 to 2002, he was with STMicroelectronics, Malaysia where he worked as product engineer. He is currently a Professor at Universiti Teknikal Malaysia Melaka (UTeM). His research interests include variety of RF/microwave devices and he has published more than 350 scientific manuscripts. He holds 8 intellectual property rights, and he has won several awards, including gold medal during several research and innovation exhibitions at the national, and international levels. He can be contacted at email: zahriladha@utem.edu.my.